

Damping of gravitational waves in 2-2-holes

Bob Holdom*

Department of Physics, University of Toronto, Toronto, Ontario, Canada M5S 1A7

A 2-2-hole is an explicit realization of a horizonless object that can still very closely resemble a black hole. An ordinary relativistic gas can serve as the matter source for a 2-2-hole solution of quadratic gravity, and this leads to a calculable area-law entropy. Here we show that it also leads to an estimate of the damping of a gravitational wave as it travels to the center of the 2-2-hole and back out again. We identify two frequency dependent effects that greatly diminish the damping. Spinning 2-2-hole solutions are not known, but we are still able to consider some spin dependent effects. The frequency and spin dependence of the damping helps to determine the possible echo resonance signal from the spinning remnants of merger events. It also controls the fate of the ergoregion instability.

I. INTRODUCTION

A 2-2-hole [1] is an example of an extremely compact horizonless object that deviates from a black hole only within some Planck-like distance from the would-be horizon. 2-2-holes exist as a class of solutions to the field equations of quadratic gravity whose only mass scale is the Planck mass. Thus the extreme compactness, as characterized by the Planck-like distance, is of purely gravitational origin. At the same time there is no upper limit on the size of these solutions, and given that they are nearly indistinguishable from black holes in many ways, there is the question of whether all black holes are actually 2-2-holes. Here we consider 2-2-holes that are gravitationally bound balls of a relativistic gas, which have been studied [2, 3] when the gravitational action consists of the Einstein term R and the Weyl-tensor-squared term $C_{\mu\nu\alpha\beta}C^{\mu\nu\alpha\beta}$ only. The Weyl term is essential for the existence of 2-2-hole solutions, and the solutions are expected to be qualitatively similar when a R^2 term is added.

These solutions are described in terms of the line element

$$ds^2 = -B(r)^2 dt^2 + A(r)^2 dr^2 + r^2 d\Omega^2 \quad (1)$$

where $A(r) = a_2 r^2 + \dots$ and $B(r) = b_2 r^2 + \dots$ near the origin. The relativistic gas with $\rho(r) = 3p(r)$ has temperature $T(r) = T_\infty B(r)^{-1/2}$. The field equations determine $A(r), B(r)$ and the combination $NT_\infty^4 m_2^2 / m_{\text{pl}}^2$, where N is $g_b + 7g_f / 8$ with g_b and g_f being the number of

* bob.holdom@utoronto.ca

bosonic and fermionic degrees of freedom in nature, and m_2 is the mass of the unstable spin-2 mode of quadratic gravity. The cumbersome field equations must be dealt with numerically, but this is sufficient to not only find these solutions but also to find the scaling behavior that relates 2-2-holes of different sizes. With the solution in hand the entropy is explicitly calculable,

$$S = \frac{(2\pi)^3}{45} N \int_0^{3GM} T(r)^3 A(r)^{1/2} r^2 dr = \zeta \frac{\text{Area}}{4G} = \zeta S_{\text{BH}} \quad (2)$$

where $\zeta \approx 0.75 N^{\frac{1}{4}} \sqrt{m_2/m_{\text{pl}}}$. The integrand is finite and it peaks at $r = 0$. The metric functions in the interior of the 2-2-hole have a strong scaling dependence on M (e.g. $a_2, b_2 \sim G/(GM)^4$) and this is responsible for the area-law scaling for S . The 2-2-hole also satisfies $ST_\infty = S_{\text{BH}} T_{\text{Hawking}}$ and so $T_\infty = T_{\text{Hawking}}/\zeta$. The total matter energy is $U = \frac{3}{8}M$.

A 2-2-hole is distinguishable from a black hole in at least one way, and that is in the behavior of low frequency gravitational waves in its vicinity. The description of a gravitational wave around a 2-2-hole reduces to a radial equation that describes a wave in a 1D cavity. Low frequencies waves tend to be trapped due to a boundary condition at one end ($r = 0$) and a potential barrier at the other end ($r = 3GM$). The cavity structure of a 2-2-hole implies a resonance spectrum [4] and possible echoes in the time domain [5–7]. But how is this picture influenced by the gravitational wave interacting with the matter inside the 2-2-hole? The properties of the gas are well determined as we have just described, and this enables this question to be addressed.

The wave and cavity description is easiest when using the tortoise radial coordinate x defined such that the line element is

$$ds^2 = B(r)^2(-dt^2 + dx^2) + r^2 d\Omega^2. \quad (3)$$

In this coordinate system waves travelling in the radial direction have unit speed and they propagate as plane waves away from the potential barrier. We can let $x = 0$ correspond to $r = 0$ and let Δx be the size of the cavity. The round trip travel time is $\Delta t = 2\Delta x = 2GML$ where L is the dimensionless length of the cavity,

$$L = 2\eta \log\left(\frac{GM}{\ell_{\text{pl}}}\right). \quad (4)$$

The cavity may be said to be stretched due to the large log associated with the Planck-like distance mentioned at the beginning. The stretching of the tortoise coordinate occurs for r where $A(r)/B(r)$ is large, and this ratio reaches a peak value at the Planck-like distance from the would-be horizon. In (4) this distance is encoded in the parameter η ; if $\eta = 1$ then this distance is the Planck length ℓ_{pl} and if $\eta = 2$ it is the much smaller proper Planck length. η describes a feature of the 2-2-hole solution that does not scale in a simple way, and numerical

determination of η for large 2-2-holes is difficult. If the resonance spectrum is observed then η will be empirically determined, as in [8].

II. DAMPING IN THE CAVITY

To study damping we start with the Hawking formula [9] for the rate of energy loss experienced by a gravitational wave traveling through a medium with shear viscosity η , (unfortunately we are already using this symbol; it will represent viscosity only in (5) and (7))

$$\frac{1}{E} \frac{dE}{dt} = -16\pi G\eta. \quad (5)$$

This simple result assumes that the wave traverses the matter as a plane wave, and we shall argue that this is a good characterization of the waves in our case. Outside a large 2-2-hole the curvatures are very small and the wave equation is dominated by a potential barrier that grows with the orbital angular momentum of the wave. The matter of interest is interior to the 2-2-hole and this range of tortoise coordinate turns out to be near the other end of the cavity, far from the potential barrier. The main effect that the interior geometry has on the wave equation is to generate a simple boundary condition at that end of the cavity. There is no divergent angular momentum barrier at $r = 0$ that would be present for a flat or any nonsingular geometry. It is precisely because the 2-2-hole has a timelike curvature singularity at $r = 0$ that there is a simple truncation of the tortoise coordinate in the wave equation, just as if a wall was introduced slightly above the horizon of a black hole (BH). There is a small difference, for the range of tortoise coordinate interior to the 2-2-hole there is a small dip in the potential in the wave equation [1], but this dip is much smaller in amplitude than the potential barrier at the other end of the cavity. Thus the waves are nearly plane waves as they traverse the matter, and so we satisfy this condition for the use of (5). When the wavelength becomes larger than the size of the matter region there is another effect that we need to account for, as we shall describe below.

A more serious deficiency of (5) is that it only applies when the frequency of the wave is much less than the collisional frequency ν_c in the medium. This is typically not the case and we shall return to a required modification of (5) shortly. ν_c is proportional to the scattering cross section between particles which in turn is proportional to the square of some effective coupling strength. We are considering a highly relativistic gas and so we can write

$$\nu_c(x) = \bar{\alpha}^2 T(x), \quad (6)$$

where $\bar{\alpha}$ is the dimensionless coupling and T is the temperature. We shall use this relation to

define $\bar{\alpha}$. The viscosity-to-entropy-density ratio will depend on this coupling,

$$\frac{\eta}{s} = \mathcal{V}(\bar{\alpha}). \quad (7)$$

Perturbative QCD for instance gives $\mathcal{V}(\bar{\alpha}) \propto 1/(\bar{\alpha}^2 \ln \bar{\alpha}^{-1})$ [10]. We might not be in the regime of small coupling and so we keep the general function in the following.

We are assuming that the system can be characterized by a single $\bar{\alpha}$. Thus we are ignoring the dependence of the coupling on the spatially varying temperature due to the energy dependence of running couplings. We also ignore the different couplings through which the different particle species in the gas can interact. It remains to refine the present work to include these effects.

The matter in the cavity has an entropy density $s(x)$, the entropy per unit area per unit x . The time t in (5) may be traded for x and we further trade x for a dimensionless coordinate $\tilde{x} = x/(GM)$ and define $\tilde{s}(\tilde{x}) = GM s(GM\tilde{x})$ so that

$$\frac{1}{E} \frac{dE}{d\tilde{x}} = -16\pi\mathcal{V}(\bar{\alpha})G\tilde{s}(\tilde{x}). \quad (8)$$

From this we can define a damping factor R_{damp} that gives the fraction of wave energy remaining after the round trip travel time $\Delta t = 2GML$,

$$R_{\text{damp}} = \exp\left(-32\pi\mathcal{V}(\bar{\alpha})G \int_0^L \tilde{s}(\tilde{x})d\tilde{x}\right). \quad (9)$$

$R_{\text{damp}} = 1$ means no damping.

The integral factor in (9) is the entropy per unit area and so from the result in (2) we have

$$\int_0^L \tilde{s}(\tilde{x})d\tilde{x} = \int_0^{\Delta x} s(x)dx = \frac{S}{\text{Area}} = \frac{\zeta}{4G}. \quad (10)$$

(10) then gives a simple result for the damping factor,

$$R_{\text{damp}} = \exp(-8\pi\mathcal{V}(\bar{\alpha})\zeta). \quad (11)$$

Both G and M have dropped out, as made possible by having a self-gravitating system. For a typical value of ζ we use 2.5, for example when $N \approx 125$ and $m_2 \approx m_{\text{pl}}$.

Since $\mathcal{V}(\bar{\alpha})$ has a theoretical lower bound of $1/(4\pi)$ [13], the result in (11) implies strong damping independent of the gravitational wave frequency ω . But this is not correct. To account for an ω that is not much less than the collisional frequency ν_c , a frequency dependent suppression factor $(1 + (\omega/\nu_c)^2)^{-1}$ should be introduced to modify the Hawking damping rate (5). This factor has been discussed recently in [14]. It is present because the shear induced by

the gravitational wave changes sign over the period of the wave, and so the time over which the particle can sample the shear is limited by this time, rather than the collisional time, when ω is larger than ν_c . Since the viscosity typically already has a $1/\nu_c$ dependence, the net effect is that the damping rate increases linearly with ν_c up to $\nu_c \approx \omega$, after which it falls like $1/\nu_c$. For a given ν_c , the damping rate is reduced by a factor ν_c^2/ω^2 when $\omega \gg \nu_c$.

For our problem we should consider the proper frequency $\omega(x) = \omega B(r(x))^{-1/2}$, and then the required ratio is $\omega(x)/\nu_c(x) = \omega/(\bar{\alpha}^2 T_\infty)$ from (6). And we have already noted that $T_\infty = T_{\text{Hawking}}/\zeta = 1/(8\pi GM\zeta)$. In terms of the dimensionless frequency $\tilde{\omega} = GM\omega$ we now have a frequency dependent damping factor,

$$R_{\text{damp}}(\tilde{\omega}) = \exp \left(-8\pi\nu(\bar{\alpha})\zeta \left[1 + \left(8\pi\tilde{\omega}\frac{\zeta}{\bar{\alpha}^2} \right)^2 \right]^{-1} \right). \quad (12)$$

This additional factor in the exponent quite dramatically reduces its magnitude as $\tilde{\omega}$ moves away from zero, and thus it reduces damping, i.e. keeps R_{damp} closer to unity. It also means that a weaker coupling $\bar{\alpha}$ implies less damping, at least for $|\tilde{\omega}|$ not very small.

There is another effect that reduces damping for very small $|\tilde{\omega}|$, when the wavelength becomes larger than the size of the matter region. A nearly trapped wave in the cavity is a superposition of the quasi-normal modes, and these QNMs are very close to being standing waves.¹ Their overall amplitude only slowly changes due to an outgoing wave of small amplitude on the outside. Standing waves have zero net energy flux across any point \tilde{x} and the energy density can vary with \tilde{x} and vanish at the nodes of the wave. If $\psi(\tilde{\omega}, \tilde{x})$ is the wave amplitude for the standing wave then the energy density profile $e(\tilde{\omega}, \tilde{x})$ is proportional to $|\psi|^2$. We define the profile to be dimensionless with $\int_0^L e(\tilde{\omega}, \tilde{x}) d\tilde{x} = L$. When the wave satisfies a Dirichlet boundary condition at $\tilde{x} = 0$, as it does for a non-rotating 2-2-hole [1], then the wave energy profile will be small near the $\tilde{x} = 0$ end of the cavity over a distance that grows with the wavelength.

The amount of wave energy being lost locally will vary from point to point, and this will be proportional to the product of the local densities of the wave energy and the matter entropy. We may define an entropy profile $\hat{s}(\tilde{x}) \propto \tilde{s}(\tilde{x})$ such that $\int_0^L \hat{s}(\tilde{x}) d\tilde{x} = 1$. The total damping rate thus has another $\tilde{\omega}$ dependent factor given by the overlap between these two profiles $\int_0^L \hat{s}(\tilde{x}) e(\tilde{\omega}, \tilde{x}) d\tilde{x}$. A numerical example of the entropy density as a function of r , $s(r)$, was shown in Fig. 18 of [2]. When r is used instead of x , most of the cavity size is compressed into a small range of r where $A(r)/B(r)$ spikes to a large finite value just slightly outside $2GM$. This spike is the source of the dominant $\log(M)$ enhanced contribution to the cavity size L . Fig. 18 of [2] shows that most of the entropy is located at smaller r . The interior contribution to L that

¹ The QNM frequencies form a discrete set $\tilde{\omega} = \tilde{\omega}_n$. For the long-lived modes the effective boundary condition from the potential barrier is close to being Neumann and so for these modes the real part of their frequencies satisfy $\tilde{\omega}_n \approx \frac{\pi}{L}(\frac{1}{2} + n)$ for integer n . When rotation is introduced, the same result applies to $\tilde{\omega}_n - \tilde{\omega}_0$.

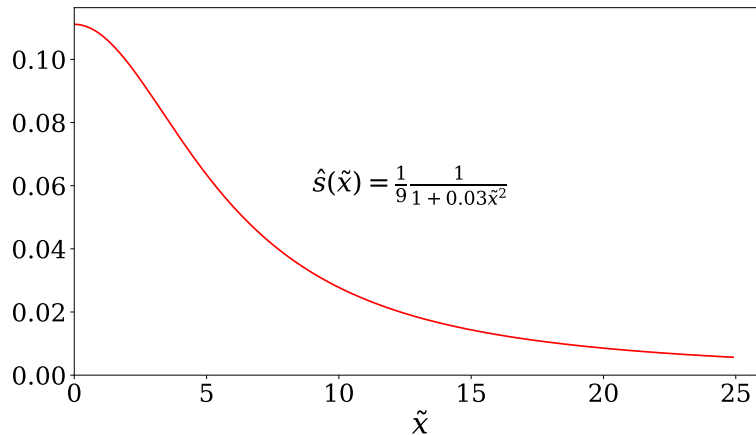


FIG. 1. The entropy profile.

is independent of $\log(M)$ is $2\sqrt{a_2/b_2} \approx 17.2$ and so Fig. 18 of [2] shows that $\hat{s}(17.2) \approx 0.1\hat{s}(0)$. From this we construct an approximate estimate of the entropy profile $\hat{s}(\tilde{x})$ as shown in Fig. 1. Since L is significantly larger than 17.2 ($L = 400$ in an example below), Fig. 1 shows that the entropy density is concentrated near the $\tilde{x} = 0$ end of the cavity.

Including the overlap integral gives our final result for the damping factor for non-rotating 2-2-holes,

$$R_{\text{damp}}(\tilde{\omega}) = \exp \left(-8\pi\nu(\bar{\alpha})\zeta \left[1 + \left(8\pi\tilde{\omega}\frac{\zeta}{\bar{\alpha}^2} \right)^2 \right]^{-1} \int_0^L \hat{s}(\tilde{x})e(\tilde{\omega}, \tilde{x})d\tilde{x} \right). \quad (13)$$

III. THE EFFECTS OF SPIN

Rotating 2-2-hole solutions, numerical or otherwise, are not known and so we cannot similarly obtain the damping result for the rotating case. But the rotating case is the one relevant for observations, with final black holes from mergers observed at LIGO-Virgo having dimensionless spins in the $\chi \gtrsim 2/3$ range. Resonance spectra for echoes have nevertheless been obtained for this case by using an approximation for rotating 2-2-holes. The approximation is a Kerr geometry that is truncated at a new boundary situated just slightly outside the horizon, with its position controlled by the parameter η as before. Then the dimensionless cavity size includes spin dependence [7, 12]

$$L = 2\eta \log\left(\frac{GM}{\ell_{\text{pl}}}\right) \left(\frac{1 + (1 - \chi^2)^{-\frac{1}{2}}}{2}\right). \quad (14)$$

Increasing spin increases the cavity size and thus the time delay and so it causes the resonances to become even more tightly spaced. We have mentioned that the wave equation for a 2-2-hole

has no angular momentum barrier at the origin $r = 0$, corresponding to $\tilde{x} = 0$. The same is true of the truncated Kerr BH where we set $\tilde{x} = 0$ at the location of the new boundary.

One way that spin affects our damping result is through the effect on the gravitational waves. We note that the gravitational wave equations for the Kerr background can be written in Sasaki-Nakamura form [15] where the waves continue to travel as plane waves away from the potential barrier. These plane waves in the cavity only differ by having an effective frequency $\omega - \omega_0$ and period $2\pi/|\omega - \omega_0|$. ω_0 is the Kerr frequency and it is proportional to χ . Thus we must replace $\tilde{\omega}$ by $\tilde{\omega} - \tilde{\omega}_0$ to have our previous discussion about frequency dependence carry over to the rotating case. We make this replacement in the damping factor (13) and so in the following we shall use $R_{\text{damp}}(\tilde{\omega} - \tilde{\omega}_0)$.

We next reconsider the wave energy profile $e(\tilde{\omega} - \tilde{\omega}_0, \tilde{x})$ in the truncated Kerr description, but as we now argue, its basic behavior remains the same. At the new boundary we can impose a condition analogous to the Dirichlet boundary condition of the non-rotating 2-2-hole. A perfectly reflecting boundary condition is imposed by requiring that the net energy flux vanish, where the latter is the difference between the ingoing and outgoing fluxes close to the boundary. Then the wave amplitude takes the form

$$\psi(\tilde{\omega}, \tilde{x}) \propto \exp(-i(\tilde{\omega} - \tilde{\omega}_0)\tilde{x}) - R(\tilde{\omega}) \exp(i(\tilde{\omega} - \tilde{\omega}_0)\tilde{x}), \quad (15)$$

where $R(\tilde{\omega})$ is a known non-negative real function [4]. From this we determine the energy density profile,

$$e(\tilde{\omega}, \tilde{x}) = \frac{4R(\tilde{\omega}) \sin((\tilde{\omega} - \tilde{\omega}_0)\tilde{x})^2 + (R(\tilde{\omega}) - 1)^2}{1 + R(\tilde{\omega})^2}. \quad (16)$$

The key point here is that $R(\tilde{\omega}_0) = 1$, and as well $R(\tilde{\omega})$ is not rapidly varying. Thus for frequencies close to $\tilde{\omega}_0$ (where the wavelength is large) the energy profile is still small where the entropy profile is large. And as $\tilde{\omega} \rightarrow \tilde{\omega}_0$ the overlap integral still tends to zero. In fact the overlap integral has little impact unless $\tilde{\omega}$ is close to $\tilde{\omega}_0$, and so there is very little dependence on the behavior of $R(\tilde{\omega})$ away from $\tilde{\omega}_0$.

Further spin dependence can enter the damping factor through the thermodynamics of the relativistic gas in a rotating 2-2-hole. In particular we need the quantities $S/\text{Area} = \zeta_1(\chi)/4G$ and $T_\infty = T_{\text{Hawking}}/\zeta_2(\chi)$. In the next section we shall present results with $\zeta_1(\chi) = \zeta_2(\chi) = \zeta$, and we comment more on this neglected and unknown spin dependence in the Conclusions.

IV. IMPLICATIONS

In Fig. 2 we compare $R_{\text{damp}}(\tilde{\omega} - \tilde{\omega}_0)$ to $R_{\text{BH}}(\tilde{\omega})$, the reflection amplitude for a Kerr black hole. $|R_{\text{BH}}| > 1$ implies superradiant amplification and a possible ergoregion instability for the

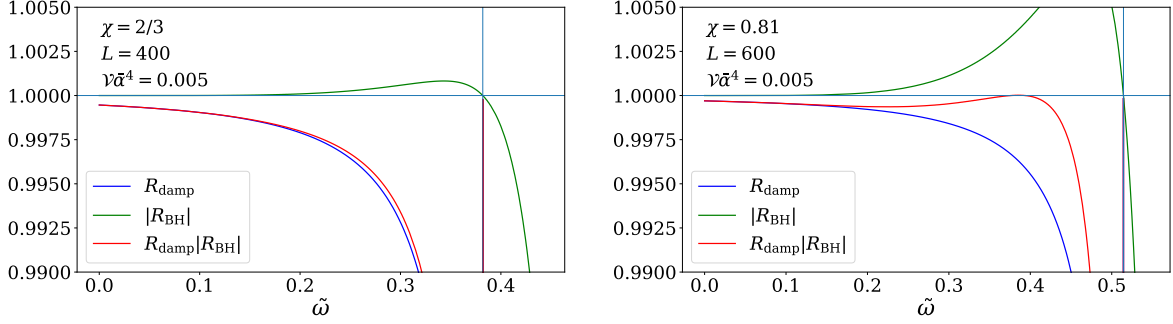


FIG. 2. The damping factor R_{damp} is compared to the Kerr black hole reflection amplitude $|R_{\text{BH}}|$ and their product. The frequency where R_{damp} spikes back up is $\tilde{\omega}_0$. The two plots compare results for different spins $\chi = 2/3$ and $\chi = 0.81$. The cavity size $L = 400$ is typical of the results in [8].

horizonless 2-2-hole. The product $|R_{\text{BH}}|R_{\text{damp}}$ is also shown in the figure and when $|R_{\text{BH}}|R_{\text{damp}} < 1$, the damping is sufficient to remove the instability. For the modeling of the spectra in [8] we used the equivalent of a constant R_{damp} (more precisely a partially absorbing wall as described by $|R_{\text{wall}}| = 0.995$ and 0.992 for $\chi = 2/3$ and 0.81 respectively). Our new more realistic $R_{\text{damp}}(\tilde{\omega} - \tilde{\omega}_0)$ quite quickly approaches unity for frequencies away from $\tilde{\omega}_0$. The $R_{\text{damp}}(\tilde{\omega} - \tilde{\omega}_0)$ dependent curves that are visible in Fig. 2 are essentially only dependent on the combination $\nu(\bar{\alpha})\bar{\alpha}^4$. When this has a value of 0.005 the left plot with $\chi = 2/3$ shows that the instability is easily removed. In the right plot with higher spin $\chi = 0.81$ we see that the same 0.005 value is now on the stability edge. Given that event GW170729 has such a spin, this sets a bound $\nu(\bar{\alpha})\bar{\alpha}^4 \gtrsim 0.005$.

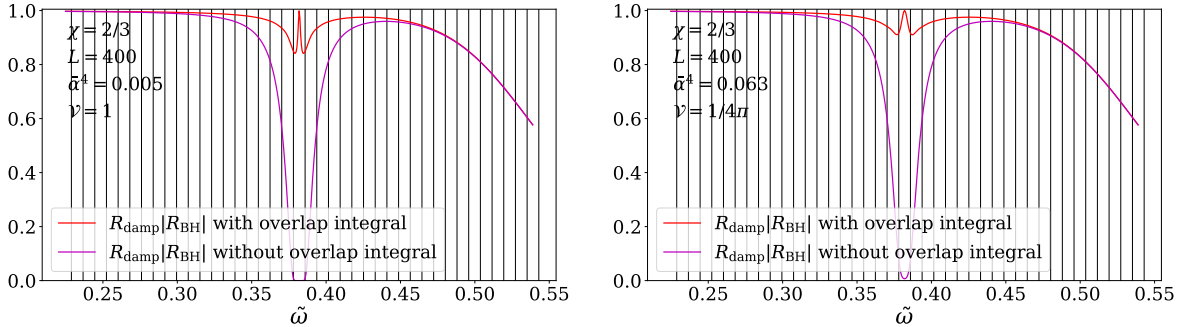


FIG. 3. The vertical and horizontal plot ranges are changed to show the effect of the overlap integral on the product $R_{\text{damp}}|R_{\text{BH}}|$. The vertical lines show QNM frequencies and their spacing π/L . The two plots show different choices of ν and $\bar{\alpha}$ with $\nu\bar{\alpha}^4 = 0.005$.

In Fig. 3 we look at the full range of the product $R_{\text{damp}}|R_{\text{BH}}|$ in a region closer to $\tilde{\omega}_0$, to see the impact of the overlap integral. We see that it significantly reduces damping close to $\tilde{\omega}_0$. The two plots show that in this region we can also see the $\bar{\alpha}$ dependence of the damping for fixed $\nu(\bar{\alpha})\bar{\alpha}^4$. The plot on the right has $\nu(\bar{\alpha}) = 1/(4\pi)$, the minimum value, and a corresponding

larger $\bar{\alpha}$, and we see that this produces the minimal amount of damping for fixed $\mathcal{V}(\bar{\alpha})\bar{\alpha}^4$.

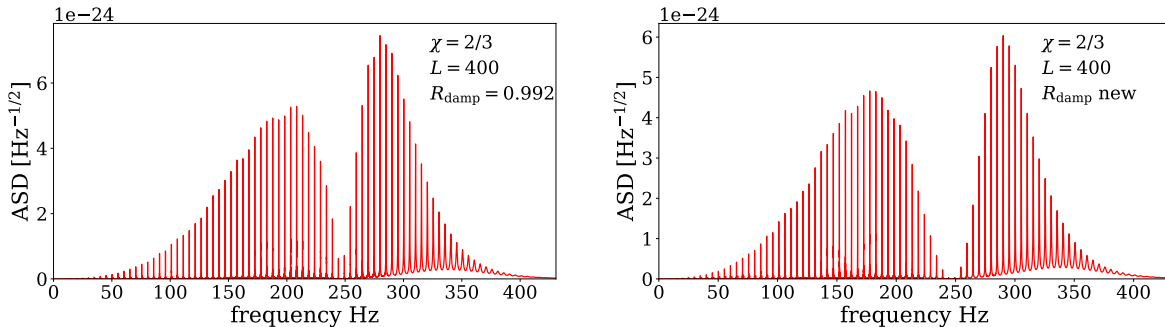


FIG. 4. The spectra are shown as amplitude spectral densities. The left plot uses a constant R_{damp} and the right plot uses our new $R_{\text{damp}}(\tilde{\omega} - \tilde{\omega}_0)$ when $\mathcal{V} = 1$ and $\bar{\alpha}^4 = 0.005$. We have converted frequencies to Hz by using a (detector frame) mass of $50M_{\odot}$. The spectra are normalized so that the peak strain in the time domain is 5×10^{-22} .

In Fig. 4 we show the effect that the new $R_{\text{damp}}(\tilde{\omega} - \tilde{\omega}_0)$ has on the observable spectrum. This is the spectrum reconstructed from the real part of the strain $\text{Re}(h(t))$ over some time duration, corresponding to 180 echoes in this example. A Greens function approach in frequency space produces a spectrum that is a product of a transfer function and a source integral, and it is from this that $h(t)$ is obtained [8, 11]. The source integral is controlled by the spectral distribution of the initial perturbation. For our example here we take a distribution proportional to $\exp(-20(\tilde{\omega} - \tilde{\omega}_0)^2)$ for a perturbation that arises inside the cavity. The source integral also brings in an explicit factor of $\omega - \omega_0$ that suppresses the spectrum around ω_0 . The two plots compare the use of our previously used constant R_{damp} to our new $R_{\text{damp}}(\tilde{\omega} - \tilde{\omega}_0)$. We see how the latter produces increased suppression around $\tilde{\omega}_0$ and less suppression elsewhere. The $\bar{\alpha}$ dependence for fixed $\mathcal{V}(\bar{\alpha})\bar{\alpha}^4$ illustrated in the Fig. 3 has very little effect since it is occurring in an already suppressed region. Thus the observed spectra essentially just constrains $\mathcal{V}(\bar{\alpha})\bar{\alpha}^4$.

V. CONCLUSIONS

A relativistic gas is the matter source for a 2-2-hole, and this displays a viscosity that can cause damping of gravitational waves. But the collisional frequency in the gas is typically less than the wave frequency and this drastically reduces the damping for those wave frequencies. For large wavelengths there is another reduction since the wave amplitude is small where the matter is located. The end result is that the remaining damping is largest for relatively low frequencies. When spin is introduced then the damping is largest for relatively low $|\omega - \omega_0|$. These are the frequencies where the superradiant effect is the largest, and so this damping will play a role in taming the ergoregion instability. We also displayed the effect of damping on the

echo resonance spectrum; the effect is not large since the spectrum is already modulated by a $|\omega - \omega_0|$ factor.

We have identified a quantity $\mathcal{V}(\bar{\alpha})\bar{\alpha}^4$ that controls the size of the damping, where $\mathcal{V}(\bar{\alpha})$ is the viscosity-to-entropy ratio and $\bar{\alpha}$ is a coupling that characterizes the gas. If we re-introduce the unknown spin dependence as mentioned at the end of Section III, then this becomes $\mathcal{V}(\bar{\alpha})\bar{\alpha}^4\zeta_1(\chi)\zeta/\zeta_2(\chi)^2$. Depending on whether this quantity increases or decreases with spin, the effect would be to weaken or strengthen the instability at high spin.

There may still be some critical value of the spin above which the ergoregion instability is not completely damped. It could be that the instability extracts energy from the rotational energy and that an 2-2-hole with a high spin will spin down to near the critical spin. The interesting question is how violent this process is. Another question is the effect of accretion on the instability. Accretion means that matter at a temperature much higher than T_∞ is entering the cavity. Until this matter equilibrates with the matter already in the cavity, it can cause gravitational wave damping unsuppressed by either of the two suppression mechanisms we have identified. It remains to determine the extent to which this can increase stability at high spins.

Our analysis constrains $\mathcal{V}(\bar{\alpha})\bar{\alpha}^4$ both from above and from below. Too large and it causes more pronounced damping in a larger region around ω_0 , which may be less consistent with the findings in [8]. Too small and the smaller damping may lead to an instability for observed high spins, e.g. for GW170729. This restriction on $\mathcal{V}(\bar{\alpha})\bar{\alpha}^4$ is interesting since it characterizes the fundamental interactions among particles at temperatures that range up to Planck energies and beyond. More theoretical knowledge of the coupling dependence of $\mathcal{V}(\bar{\alpha})$ could then separately constrain both this ratio and the value of the effective coupling.

ACKNOWLEDGMENTS

This research was supported in part by the Natural Sciences and Engineering Research Council of Canada.

-
- [1] B. Holdom and J. Ren, “Not quite a black hole”, Phys. Rev. D **95**, no. 8, 084034 (2017). [arXiv:1612.04889 [gr-qc]].
 - [2] B. Holdom, “A ghost and a naked singularity; facing our demons,” arXiv:1905.08849 [gr-qc].
 - [3] J. Ren, “Anatomy of a thermal black hole mimicker,” Phys. Rev. D **100**, no. 12, 124012 (2019) [arXiv:1905.09973 [gr-qc]].
 - [4] R. S. Conklin, B. Holdom and J. Ren, “Gravitational wave echoes through new windows”, Phys. Rev. D **98**, no. 4, 044021 (2018) [arXiv:1712.06517 [gr-qc]].

- [5] V. Cardoso, E. Franzin and P. Pani, “Is the gravitational-wave ringdown a probe of the event horizon?,” *Phys. Rev. Lett.* **116**, no. 17, 171101 (2016) Erratum: [*Phys. Rev. Lett.* **117**, no. 8, 089902 (2016)] [arXiv:1602.07309 [gr-qc]].
- [6] V. Cardoso, S. Hopper, C. F. B. Macedo, C. Palenzuela and P. Pani, “Gravitational-wave signatures of exotic compact objects and of quantum corrections at the horizon scale”, *Phys. Rev. D* **94**, no. 8, 084031 (2016) [arXiv:1608.08637 [gr-qc]].
- [7] J. Abedi, H. Dykaar and N. Afshordi, “Echoes from the Abyss: Tentative evidence for Planck-scale structure at black hole horizons”, *Phys. Rev. D* **96**, no. 8, 082004 (2017) [arXiv:1612.00266 [gr-qc]].
- [8] B. Holdom, “Not quite black holes at LIGO,” *Phys. Rev. D* **101**, no.6, 064063 (2020) [arXiv:1909.11801 [gr-qc]].
- [9] S. Hawking, “Perturbations of an expanding universe,” *Astrophys. J.* **145** 544 (1966).
- [10] P. B. Arnold, G. D. Moore and L. G. Yaffe, “Transport coefficients in high temperature gauge theories. 1. Leading log results,” *JHEP* **11**, 001 (2000) [arXiv:hep-ph/0010177 [hep-ph]].
- [11] R. S. Conklin and B. Holdom, “Gravitational wave echo spectra,” *Phys. Rev. D* **100**, no. 12, 124030 (2019) [arXiv:1905.09370 [gr-qc]] (and references therein).
- [12] V. Cardoso and P. Pani, “The observational evidence for horizons: from echoes to precision gravitational-wave physics”, *Nat. Astron.* **1**, 586 (2017) [arXiv:1707.03021 [gr-qc]].
- [13] P. Kovtun, D. T. Son and A. O. Starinets, “Viscosity in strongly interacting quantum field theories from black hole physics,” *Phys. Rev. Lett.* **94**, 111601 (2005) [hep-th/0405231].
- [14] A. Loeb, “Upper Limit on the Dissipation of Gravitational Waves in Gravitationally Bound Systems,” *Astrophys. J.* **890**, no. 2, L16 (2020) [arXiv:2001.01730 [astro-ph.HE]].
- [15] M. Sasaki and T. Nakamura, “Gravitational Radiation From a Kerr Black Hole. 1. Formulation and a Method for Numerical Analysis,” *Prog. Theor. Phys.* **67**, 1788 (1982).